



**HAL**  
open science

## Role of enteric glial cells in the toxicity of phycotoxins: Investigation with a tri-culture intestinal cell model

Océane Reale, Dorina Bodi, Antoine Huguet, Valérie Fessard

### ► To cite this version:

Océane Reale, Dorina Bodi, Antoine Huguet, Valérie Fessard. Role of enteric glial cells in the toxicity of phycotoxins: Investigation with a tri-culture intestinal cell model. *Toxicology Letters*, 2021, 351, pp.89-98. 10.1016/j.toxlet.2021.08.013 . anses-03378478

**HAL Id: anses-03378478**

**<https://anses.hal.science/anses-03378478>**

Submitted on 16 Oct 2023

**HAL** is a multi-disciplinary open access archive for the deposit and dissemination of scientific research documents, whether they are published or not. The documents may come from teaching and research institutions in France or abroad, or from public or private research centers.

L'archive ouverte pluridisciplinaire **HAL**, est destinée au dépôt et à la diffusion de documents scientifiques de niveau recherche, publiés ou non, émanant des établissements d'enseignement et de recherche français ou étrangers, des laboratoires publics ou privés.



Distributed under a Creative Commons Attribution - NonCommercial 4.0 International License

1 *Article*

## 2 **Role of enteric glial cells in the toxicity of phycotoxins:** 3 **investigation with a tri-culture intestinal cell model**

4 **Océane Reale<sup>1</sup>, Dorina Bodi<sup>2</sup>, Antoine Huguet<sup>1</sup> and Valérie Fessard<sup>1\*</sup>**

5 <sup>1</sup>: Toxicology of Contaminants Unit, French Agency for Food, Environmental and Occupational Health &  
6 Safety (Anses), Fougères Laboratory, 10B rue Claude Bourgelat, 35306 Fougères cedex, France

7 <sup>2</sup>: Unit Contaminants, German Federal Institute for Risk Assessment, Department Safety in the Food Chain,  
8 Max-Dohrn-Str. 8-10, 10589 Berlin, Germany

9  
10 \* Correspondence: [valerie.fessard@anses.fr](mailto:valerie.fessard@anses.fr)

11 **Abstract:** Lipophilic phycotoxins are secondary metabolites produced by phytoplankton. They can accumulate  
12 in edible filtering-shellfish and cause human intoxications, particularly gastrointestinal symptoms. Up to now,  
13 the *in vitro* intestinal effects of these toxins have been mainly investigated on simple monolayers of intestinal  
14 cells such as the enterocyte-like Caco-2 cell line. Recently, the combination of Caco-2 cells with mucus  
15 secreting HT29-MTX cell line has been also used to mimic the complexity of the human intestinal epithelium.  
16 Besides, enteric glial cells (EGC) from the enteric nervous system identified in the gut mucosa have been  
17 largely shown to be involved in gut functions. Therefore, using a novel model integrating Caco-2 and  
18 HT29-MTX cells co-cultured on inserts with EGC seeded in the basolateral compartment, we examined the  
19 toxicological effects of two phycotoxins, pectenotoxin-2 (PTX2) and okadaic acid (OA). Cell viability,  
20 morphology, barrier integrity, inflammation, barrier crossing, and the response of some specific glial markers  
21 were evaluated using a broad set of methodologies. The toxicity of PTX2 was depicted by a slight decrease of  
22 viability and integrity as well as a slight increase of inflammation of the Caco-2/HT29-MTX co-cultures. PTX2  
23 induced some modifications of EGC morphology. OA induced IL-8 release and decreased viability and  
24 integrity of Caco-2/HT29-MTX cell monolayers. EGC viability was slightly affected by OA. The presence of  
25 EGC reinforced barrier integrity and reduced the inflammatory response of the epithelial barrier following OA  
26 exposure. The release of GDNF and BDNF gliomediators by EGC could be implicated in the protection  
27 observed.

28 **Keywords:** pectenotoxin-2, okadaic acid, Caco-2 cells, HT29-MTX cells, enteric glial cells, toxicity  
29

### 30 **1. Introduction**

31 Phycotoxins are secondary metabolites produced by marine planktonic micro-algae that can accumulate  
32 especially in filter-feeding bivalves such as clams, mussels and scallops (Reguera et al. 2014, EFSA Journal  
33 2009). Due to the worldwide expansion of harmful algal blooms as well as the emergence of new toxin analogs,  
34 phycotoxins remain an ecological, economic and public health concern that require consistent monitoring over  
35 the world (EFSA Journal 2009). Among lipophilic phycotoxins, some including okadaic acid (OA) and analogs  
36 have been reported to provoke human intoxications depicted by gastrointestinal symptoms such as nausea,  
37 diarrhea, abdominal pains and vomiting (EFSA Journal 2008). For other few like pectenotoxins (PTX), acute  
38 toxic effects were described in rodents (Ishige et al. 1988; Ito 2006; Ito et al. 2008), but no human intoxications

39 have been proven so far. Although *in vivo* studies are still the gold standard for toxicity evaluation, *in vivo* data  
40 on phycotoxins are limited due to toxin cost and availability, besides ethical reasons. Therefore, *in vitro*  
41 intestinal human cell models can be a simple, rapid and reproducible tool for a deeper investigation of  
42 phycotoxin effects on intestine. So far, only the enterocyte-like Caco-2 cell line has been extensively used for  
43 this purpose. Nevertheless, goblet cells, generally mimicked by the HT29-MTX cell line, are also potential key  
44 players as they are the second more present cells of the human intestinal epithelium and produce a mucus layer  
45 with a protecting role (Forstner, 1994). Thereby, co-cultures of Caco-2/HT29-MTX cells have already been  
46 used to study the effects of various types of toxins such as mycotoxins (Ly et al. 2014) and more recently  
47 phycotoxins such as OA and PTX2 (Reale et al 2020).

48 Concerning lipophilic phycotoxins, OA has been shown to induce intestinal toxicity in mice with cell  
49 detachment, fluid accumulation, villous atrophy, inflammation and dilatation of the intestinal tract (Ito et al.  
50 2004; Ito et al. 2002; Wang et al. 2012). Interestingly, on both intestinal Caco-2 and HT29-MTX cell  
51 monocultures, OA has been shown to induce a decrease of cell viability, activate apoptosis (caspase-3) and  
52 inflammation (NF- $\kappa$ B) as well as to disturb the cell cycle (Ferron et al., 2014). OA increased also the  
53 paracellular permeability of intestinal T84 and Caco-2 cells monolayer (Ehlers et al., 2011; Dietrich et al.,  
54 2019). In contrast to OA, PTX2 induced only moderate damage on the intestinal epithelium with a fast recovery  
55 in mice (Ito et al. 2008; Suzuki et al. 2006; Terao et al. 1986). *In vitro*, on differentiated Caco-2 cells, PTX2 did  
56 not induce reduction of viability, neither IL-8 release and oxidative stress (Alarcan et al., 2019). Nevertheless,  
57 an alteration of Caco-2 cells monolayer integrity has been reported with PTX2 (Hess et al., 2007) while PTX6,  
58 an analogue of PTX2, induced inhibition of F-actin polymerisation on rabbit primary enterocytes (Ares et al.,  
59 2005). Recently, we found that both toxins induced cytotoxicity and affected Caco-2/HT29-MTX cell  
60 monolayer integrity (Reale et al., 2020). However, non-epithelial cell types of the intestinal barrier can  
61 potentially contribute to the outcome of intestinal symptoms through their interaction with epithelial cells.  
62 Among these non-epithelial cells, enteric glial cells (EGC), belonging to the enteric nervous system, maintain a  
63 physiological crosstalk with intestinal epithelial cells for the regulation of homeostasis, gut functions, and  
64 intestinal barrier permeability through the release of various gliomediators (Neunlist et al. 2014; Neunlist et al.  
65 2013; Yu and Li 2014). Indeed, rodent models with EGC depletion have shown a clear disruption of the  
66 intestinal barrier with inflammation, persistent diarrhea, and loss of integrity (Bush et al., 1998; Langness et al.,  
67 2017; Ochoa-Cortes et al., 2016). Therefore, EGC could modulate the intestinal barrier response to OA and  
68 PTX2. Interestingly, EGC in monoculture have been shown to be sensitive to OA and PTX2 (Reale et al., 2019).

69 In the present study, we evaluated the toxicity of OA and PTX2 using a Caco-2/HT29-MTX/EGC cells  
70 tri-culture model. Various approaches were used to investigate cell viability (neutral red uptake (NRU) assay),  
71 morphology, barrier integrity (transepithelial electrical resistance (TEER) evaluation and lucifer yellow (LY)  
72 crossing), inflammation (ELISA), toxins barrier crossing (LC-MS/MS) and response of specific glial markers ,  
73 (RT-qPCR, and High Content Analysis (HCA)).

74

75

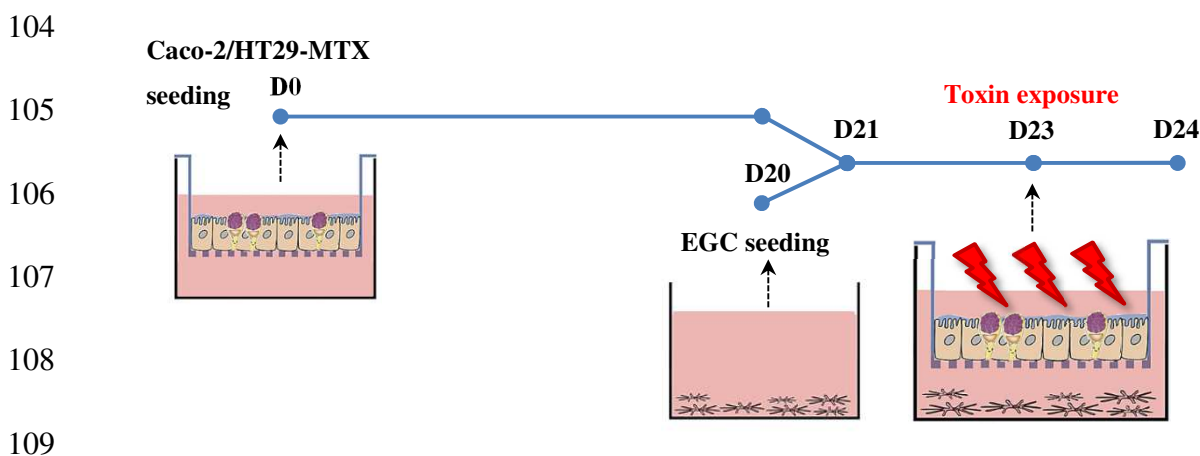
## 76 2. Materials and Methods

### 77 2.1 Chemicals

78 Cell culture products were purchased from Gibco (Cergy-Pontoise, France). Bovine serum albumin (BSA),  
79 Tween 20, TritonX100, neutral red, lucifer yellow and HEPES were supplied by Sigma-Aldrich (Saint Quentin  
80 Fallavier, France). Monoclonal IL-8, biotinylated monoclonal IL-8 antibodies, SuperBlock blocking buffer,  
81 streptavidin peroxidase, TNF $\alpha$  and TMB were purchased from ThermoFisher Scientific (Waltham, MA). For *in*  
82 *vitro* assays, PTX2 and OA, dissolved in methanol (MeOH), were purchased from the National Research  
83 Council Canada (NRCC, Halifax, Nova Scotia, Canada). For LC-MS/MS analysis, OA standard dissolved in  
84 MeOH was supplied by Enzo Life Science (Lörrach, Germany). Acetonitrile (ACN) and MeOH were purchased  
85 from Merck KGaA both of LC-MS/MS grades (Darmstadt, Germany).

### 86 5.2 Cell culture and toxins exposure

87 Caco-2 cells (HTB-37), obtained from the American Type Culture Collection (ATCC) (Manassas, VA), were  
88 maintained in Minimum Essential Medium containing 5.5 mM D-glucose, Earle's salts and 2 mM  
89 L-alanyl-glutamine (MEM GlutaMAX) supplemented with 10% fetal bovine serum (FBS), 1% non-essential  
90 amino acids, 50 IU/mL penicillin and 50  $\mu$ g/mL streptomycin at 37°C and 5% CO<sub>2</sub>. HT29-MTX (kindly  
91 provided by Dr T. Lesuffleur, Paris, France) were cultured in Dulbecco's Modified Eagle's Medium with high  
92 glucose (DMEM) supplemented with 10% inactivated FBS, 50 IU/mL penicillin and 50  $\mu$ g/mL streptomycin  
93 (complete DMEM) at 37°C and 5% CO<sub>2</sub>. The rat EGC (CRL2690), obtained from the ATCC, were grown in  
94 DMEM supplemented with 10% FBS, 50 IU/mL penicillin and 50  $\mu$ g/mL streptomycin at 37 °C and 5% CO<sub>2</sub>.  
95 For tri-culture experiments, first Caco-2 and HT29-MTX cells (3:1) were seeded at 157,000 cells/cm<sup>2</sup>  
96 in complete DMEM in 12-well and 24-well inserts (polyester membrane, 0.4  $\mu$ m pore size; Corning, USA) which  
97 were used for qPCR assays, and for cytotoxicity and monolayer integrity assays, respectively. Culture medium  
98 was changed three times each week up to 21 days post-seeding (Figure 1). At D20, EGC were seeded at 30,000  
99 cells/cm<sup>2</sup> in 12-well and 24-well plates. At D21, inserts containing Caco-2/HT29-MTX cells were transferred  
100 into the plates containing EGC. At D23, cells were exposed 24 hours to toxins loaded in the apical compartment  
101 in FBS-free complete DMEM. Concentrations ranged from 50 nM to 260 nM for PTX2 and from 100 nM to 320  
102 nM for OA. The maximal tolerated concentration of MeOH (5%) was chosen for the top concentration of each  
103 toxin, and this experimental condition was included in each experiment as vehicle control.



110

111 **Figure 1. Schematic representation of the tri-culture experimental design.** Caco-2 and HT29-MTX cells  
112 (3:1) were seeded on inserts and grown until D21. EGC were seeded at D20 in plates and grown until D21. At  
113 D21, inserts containing Caco-2/HT29-MTX cells were transferred into the plates containing EGC. At D23,  
114 apical treatment with the toxins was performed.

### 115 *2.3 Neutral red uptake assay and morphological observations*

116 After 24 hrs of treatment, inserts containing Caco-2/HT29-MTX cells were placed in a novel 12-well plates in  
117 order to process to the NRU assay, separately from EGC. Cell morphological changes of EGC were observed by  
118 phase contrast microscopy (Leica Microsystems, Wetzlar, Germany). Cytotoxicity was assessed by the NRU  
119 assay for Caco-2/HT29-MTX co-cultures and for EGC as previously described (Reale et al. 2019). Three  
120 independent experiments were performed and, for each experiment, the value was expressed relative to that of  
121 the vehicle control.

### 122 *2.4 IL-8 release*

123 The levels of interleukin-8 (IL-8) released in the apical compartment were determined as previously described  
124 (Tarantini et al. 2015). Three independent experiments with three technical replicates per experiment were  
125 performed.

### 126 *2.5 Monolayer integrity assays*

#### 127 *2.5.1 TEER measurement*

128 The trans-epithelial electrical resistance (TEER) of the Caco-2/HT29-MTX co-cultures was measured to  
129 evaluate the monolayer integrity before and after the 24-hrs treatment with toxins loaded in the apical  
130 compartment. The TEER measurements and analyses were performed as previously described (Reale et al.,  
131 2020). Only Caco-2/HT29-MTX monolayers with TEER > 130  $\Omega$ .cm<sup>2</sup> were considered as intact. Three  
132 independent experiments were performed.

#### 133 *2.5.2 LY crossing*

134 After toxin treatment, the ability of LY to cross the Caco-2/HT29-MTX monolayers was determined as  
135 previously described (Reale et al., 2020). The amount of LY in the basolateral compartment was expressed  
136 relative to that of the amount loaded in the apical compartment, and then expressed per hour. Three independent  
137 experiments were performed.

#### 138 *2.5.3 ZO-1 immunofluorescence*

139 After 24 hrs of treatment with toxins, the detection of ZO-1 in Caco-2/HT29-MTX co-cultures was performed  
140 by immunofluorescence as previously described (Ferron et al. 2014) with the following modifications.  
141 Antibodies used were anti-rabbit ZO-1 (1/200, ThermoFisher Scientific) and goat anti-rabbit IgG (H+L) Alexa  
142 Fluor®647 (1/1000, ab150079, Abcam, Cambridge, UK). Cell identification was performed using DAPI  
143 (Sigma-Aldrich) labelling. The semi-permeable membranes were carefully removed from the insert and  
144 mounted onto a glass slide using an aqueous mounting fluid. Two independent experiments were performed.

### 145 *2.6 RT-qPCR*

146 After 24 hrs of treatment with PTX2 (100, 150, and 200 nM) and OA (75, 125, and 175 nM), genes expression  
147 in Caco-2/HT29-MTX cells in one hand and in EGC in the other hand was evaluated as previously described  
148 (Reale et al. 2019) with the following modifications. For Caco-2/HT29-MTX cells, reverse transcription was  
149 performed with 2.5 µg of total RNA, and quantitative PCR reactions were carried out in a total volume of 5 µL  
150 containing 8.33 ng cDNA. For EGC analysis, reverse transcription was performed with 2 µg of total RNA, and  
151 quantitative PCR reactions were carried out in a total volume of 5 µL containing 6.67 ng cDNA. All primers  
152 were purchased from Sigma-Aldrich and additional information on primers are listed in Table S1 (for  
153 Caco-2/HT29-MTX cells) and S2 (for EGC). Using NormFinder software, the genes *RPLP0* and *ACTB* were  
154 chosen as reference gene for Caco-2/HT29-MTX cells and for EGC, respectively, since they did not exhibit any  
155 significant variation of expression among the samples. Three independent experiments were performed.

### 156 2.7 LC-MS/MS analysis

157 After 24 hrs of treatment with phycotoxins, the basolateral compartments were harvested from the plates  
158 dedicated to integrity testing and stored into glass vials at -20°C until analysis. Toxin analysis was conducted on  
159 a TSQ Quantiva mass spectrometer system coupled to an Ultimate 3000 Ultra High Performance Liquid  
160 Chromatography (both Thermo Fisher Scientific, Bremen, Germany). Chromatographic separation was carried  
161 out on a Thermo Hypersil Gold C18 column (Thermo Fisher, Bremen, Germany) (150 × 2.1 mm, 1.9 µm) using  
162 two mobile phase preparations, consisting of mobile phase (A), 100% water, and mobile phase (B), 5% water  
163 and 95% acetonitrile. Both mobile phases contained 2 mM of ammonium formate and 50 mM of formic acid.  
164 The gradient conditions were as follows: from 0 to 1 min, 90% of mobile phase A, then from 1 to 6 min, linear  
165 ramp from 90% to 10% of mobile phase A which was held for 6 min, then ramp back in 0.5 min to initial  
166 conditions and held for 5 min to re-equilibrate the system. The flow rate was set at 0.2 mL/min, the injection  
167 volume was 5 µL, and the column oven was maintained at 40°C. The mass spectrometer was operated in  
168 negative mode. The following source parameters were used: sheath gas flow rate: 40 arb; auxiliary gas flow  
169 rate: 10 arb; sweep gas flow rate: 1 arb; ion spray voltage: 4.0 kV in positive mode and 2.2 kV in negative mode;  
170 capillary temperature: 335°C. The analytes were detected by Selected Reaction Monitoring (SRM). For analyte  
171 identification and quantification, toxin specific transitions from molecular ions to product ions were chosen:  
172 803.5>563.3 (CE: -40 V) and 803.5>785.5 (CE: -34 V) for identification and 803.5>255.0 (CE: -45 V) for  
173 quantification. The mass spectrometer was operated in unit resolution (0.7 amu). Based on S/N, LOD and LOQ  
174 were estimated at 60 and 200 pg/mL. OA was quantified using a calibration curve with toxin standards at 0, 1, 2,  
175 3, 4, 5, 10, 20, 30, 50 ng/mL (OA). OA standard was solved in cell culture medium (complete DMEM without  
176 FBS). Percentage of crossing was determined as the percentage of the absolute amount of toxin detected in the  
177 basolateral compartment among the theoretical toxin amount loaded in the apical compartment.

### 178 2.8 Glial cell markers

179 After 24 hrs of treatment, the immunofluorescence detection of iNOS and GDNF was performed as previously  
180 described (Reale et al. 2019) with the following modifications. Antibodies were purchased from Abcam: mouse  
181 anti-iNOS (1/350, ab49999), rabbit anti-GDNF (1/200, ab18956), goat anti-mouse IgG (H&L) Alexa Fluor®  
182 555 (1/1000, ab150114) and goat anti-rabbit IgG (H&L) Alexa Fluor® 647 (1/1000, ab150079). The Target  
183 Activation Module of the BioApplication software (Arrayscan VTI HCS Reader, Thermo Scientific) was used  
184 to quantify iNOS and GDNF in the cytoplasm. Cytomix (50 ng/ml TNFα (BD Pharmingen Biosciences) + 50

185 ng/ml IL1 $\beta$  (Sigma Aldrich) + 50 ng/mL IFN $\gamma$  (Thermo Fisher, Waltham, MA, USA)) was used as positive  
 186 control for iNOS. For each well, 6 fields (20X magnification) were analyzed. Cell counts were performed using  
 187 nuclear DAPI labelling. Three independent experiments were performed.

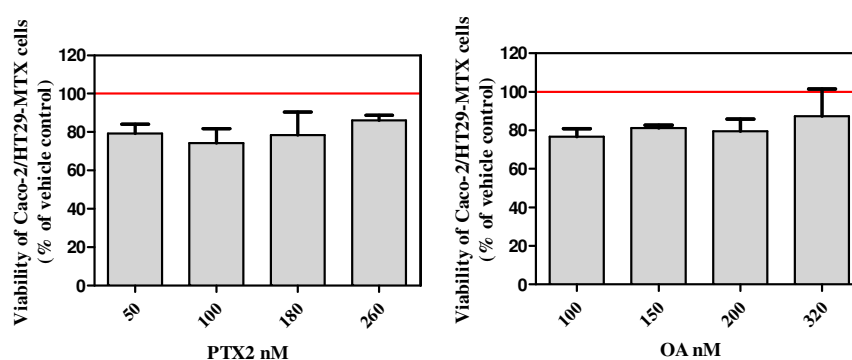
## 188 2.9 Statistics

189 GraphPad Prism software was used for statistical analyses. One sample T-test was performed for cytotoxicity  
 190 and HCA assays. An analysis of variance (ANOVA) was performed for TEER, LY crossing, IL-8 release and  
 191 RT-qPCR assays, and, if the effect of concentration was significant ( $P < 0.05$ ), the values were compared to the  
 192 control using the Dunnett's test. Differences were declared significant at  $P < 0.05$ . The values presented are  
 193 means  $\pm$  SEM.

## 194 3. Results

### 195 3.1. Cytotoxic effects of PTX2 and OA on Caco-2/HT29-MTX co-cultures

196 After 24 hrs of apical treatment with the toxins, a slight decrease of cell viability (around 20%) was observed in  
 197 Caco-2/HT29-MTX co-cultures from the lowest tested concentration (50 nM PTX2 and 100 nM OA) (Figure  
 198 2).



199

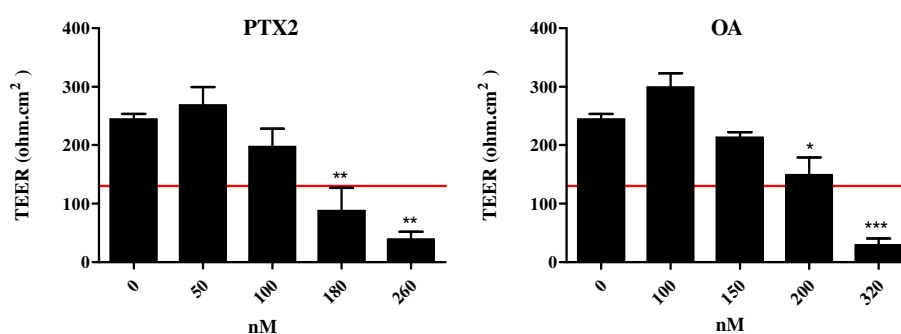
200 **Figure 2. Cytotoxicity on Caco-2/HT29-MTX cells after a 24 hrs apical treatment with PTX2 and OA.**

201 Cytotoxicity was measured by the neutral red uptake (NRU) assay. Values are presented as means  $\pm$  SEM and  
 202 expressed as percentages relative to the vehicle control (red line). Three independent experiments were  
 203 performed.

### 204 3.2. Caco-2/HT29-MTX co-cultures monolayer integrity

#### 205 3.2.1 TEER and LY permeability

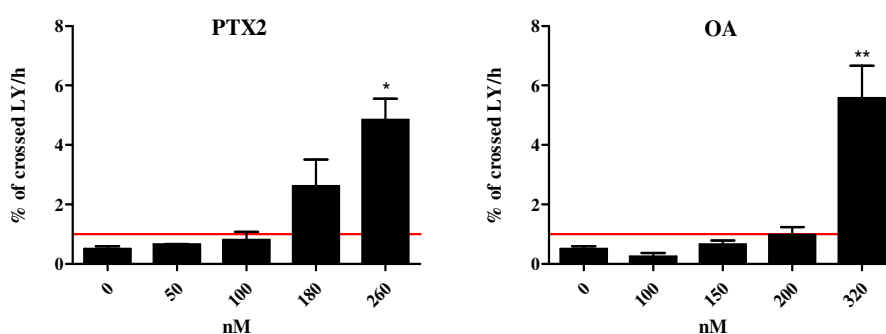
206 The TEER value for the vehicle control (with EGC) was on average  $244 \pm 16$  ohm.cm<sup>2</sup> whereas it was around  
 207 162 ohm.cm<sup>2</sup> at D21 before to add EGC. The integrity of the Caco-2/HT29-MTX co-cultures monolayers was  
 208 significantly affected after 24 hrs treatment with the toxins: -64% and -83% at 180 and 260 nM PTX2  
 209 respectively, and -87% at 320 nM OA (Figure 3). Although 200 nM OA induced a significant decrease of  
 210 TEER, the value remained above 130 ohm.cm<sup>2</sup>, which was considered as not affecting the monolayer integrity.



211

212 **Figure 3. TEER measurement on Caco-2/HT29-MTX co-cultures monolayer in the presence of EGC**  
 213 **after 24 hrs apical treatment with PTX2 and OA.** Values are presented as means  $\pm$  SEM. Red line: 130  
 214 ohm.cm<sup>2</sup>. Caco-2/HT29-MTX co-cultures monolayers with a TEER > 130 ohm.cm<sup>2</sup> were considered as intact.  
 215 Three independent experiments were performed. \*, \*\*, \*\*\*: value significantly different from the vehicle  
 216 control ( $P < 0.05$ ,  $P < 0.01$  and  $P < 0.001$  respectively).

217 For the vehicle control, the rate of LY that crossed into the basolateral compartment was on average  $0.51 \pm 0.10$   
 218 %/h (Figure 4). This value was significantly increased by apical treatment with both phycotoxins, reaching 4.80  
 219 and 5.60 %/h with 260 nM PTX2 and 320 nM OA respectively.



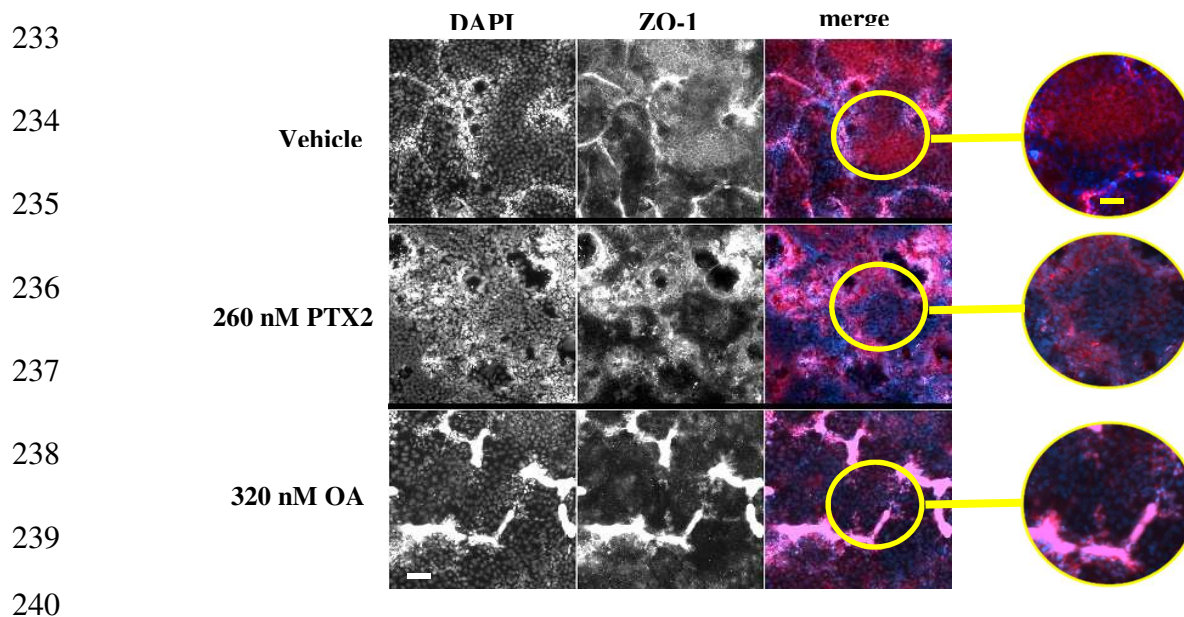
220

221 **Figure 4. LY crossing through Caco-2/HT29-MTX co-cultures monolayer in the presence of EGC after**  
 222 **24 hrs apical treatment with PTX2 and OA.** Values are presented as means  $\pm$  SEM, and expressed as  
 223 percentage of LY that crossed into the basolateral compartment per hour. Red line: 1%/h. Caco-2/HT29-MTX  
 224 co-cultures monolayers with a value of LY/h < 1% were considered as intact. Three independent experiments  
 225 were performed. \*, \*\*: value significantly different from the vehicle control ( $P < 0.01$  and  $P < 0.001$   
 226 respectively).

### 227 3.2.2. ZO-1 immunofluorescence

228 In the vehicle control cells, ZO-1 staining was mainly distributed at the cell border (Figure 5). Treatment up to  
 229 260 nM PTX2 and up to 320 nM OA reduced the staining intensity of ZO-1 along the borders. Areas without  
 230 cells were observed with PTX2 treatment while with OA, an accumulation of ZO-1 was observed at the top of  
 231 the cell monolayer.

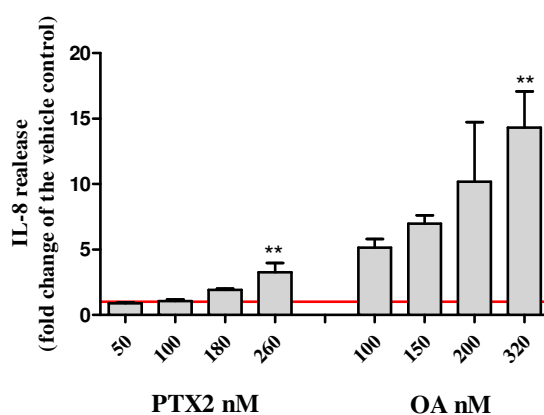
232



241 **Figure 5. Immunofluorescence localization of zonula occludens 1 (ZO-1) in the Caco-2/HT29-MTX**  
 242 **co-cultures monolayer in the presence of EGC after 24 hrs apical treatment with PTX2 and OA. ZO-1**  
 243 **(red) and DAPI (blue) nucleus staining were carried out by immunocytochemistry. Each image is representative of**  
 244 **three independent experiments. Scale bar (white) = 60  $\mu$ m and scale bar (yellow) = 30  $\mu$ m.**

### 245 3.3. Inflammatory response of Caco-2/HT29-MTX co-cultures

246 After 24 hrs treatment, a concentration-dependent increase of IL-8 release in the apical compartment was  
 247 observed for both phycotoxins (Figure 6). The IL-8 concentration increased significantly up to 3.3-fold with  
 248 260 nM PTX2 and up to 14-fold with 320 nM OA compared to the vehicle control.



249

250 **Figure 6. IL-8 release of Caco-2/HT29-MTX co-cultures in the presence of EGC after a 24 hrs apical**  
 251 **treatment with PTX2 and OA. IL-8 release was expressed as fold change compared to the vehicle control**  
 252 **set to 1 (red line). IL-8 release in the vehicle control was 79.2  $\pm$  5.6 pg/mL. Values are presented as means  $\pm$  SEM.**  
 253 **Three independent experiments were performed. \*\*: value significantly different from the vehicle control ( $P <$**   
 254 **0.01).**

### 255 3.4. Modulation of genes expression following treatment with PTX2 and OA on Caco-2/HT29-MTX

256 Additional investigations were done through expression analysis of key genes involved in inflammation,  
 257 adherence, transport and mucus production for Caco-2/HT29-MTX co-cultures (Table 1). For

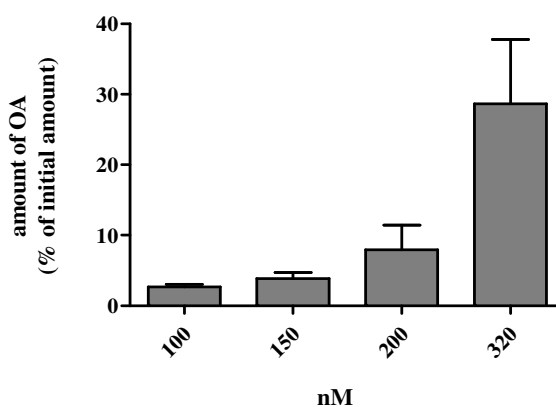


<i>SLCO1A2</i>							
<i>ABCC1</i>							
<i>ABCC5</i>					*	**	
<i>ABCC3</i>							

273

274 *3.5 Transport of OA through the Caco-2/HT29-MTX co-cultures*

275 The amounts of OA found in the basolateral compartment were quantified 24 hrs after loading the toxins into  
 276 the apical compartment. OA crossed the Caco-2/HT29-MTX co-cultures in a concentration-dependent manner  
 277 and reached 8% at 200 nM and 28.7% at 320 nM (Figure 7).

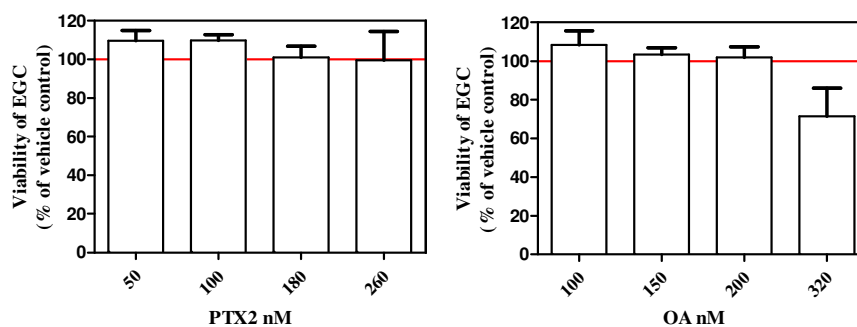


278

279 **Figure 7. Basolateral relative quantities of OA following 24 hrs apical treatment of Caco-2/HT29-MTX**  
 280 **co-cultures monolayer in the presence of EGC.** Values are expressed as percentage of the initial amount  
 281 loaded in the apical compartment and are presented as means  $\pm$  SEM. Three independent experiments were  
 282 performed.

283 *3.6. Cytotoxic and morphological effects of PTX2 and OA on EGC*

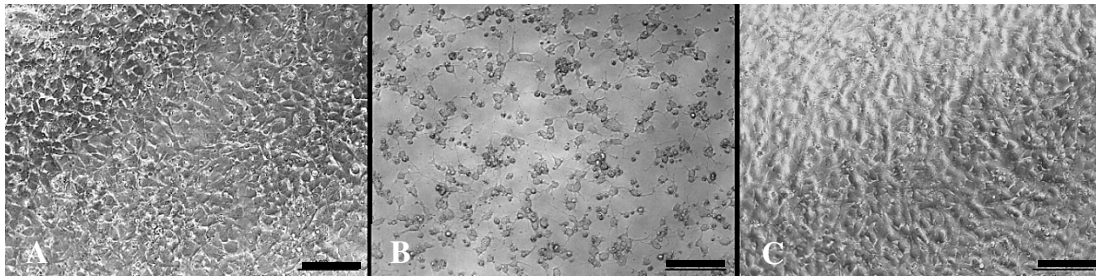
284 While treatment of PTX2 up to 260 nM did not affected the viability of basolateral EGC, a decrease of  
 285 viability (28%) was observed with OA but only at the highest concentration (320 nM) (Figure 8).



286

287 **Figure 8. Cytotoxicity on EGC after a 24 hrs apical treatment with PTX2 and OA.** Cytotoxicity was  
 288 measured by the neutral red uptake (NRU) assay. Values are presented as means  $\pm$  SEM and expressed as  
 289 percentages relative to the vehicle control (red line). Three independent experiments were performed.

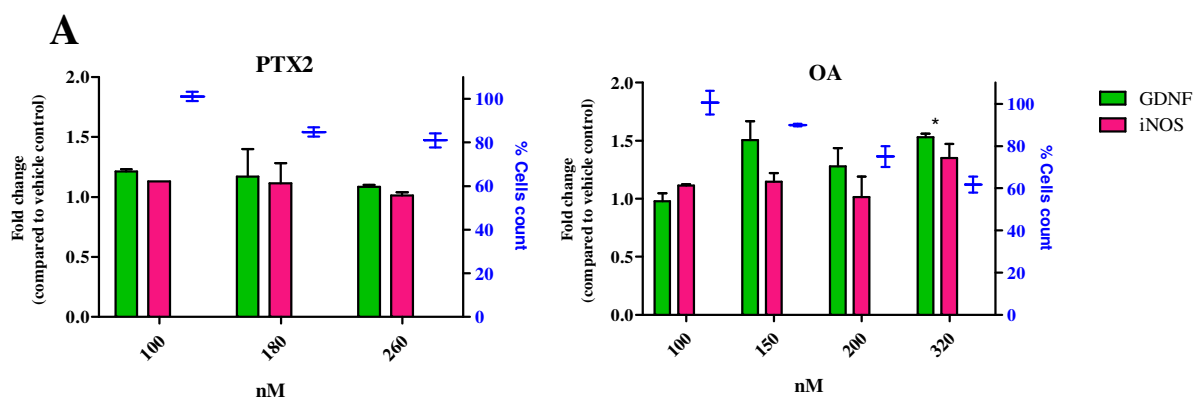
290 The morphology of EGC was observed after 24 hrs of apical treatment with phycotoxins (Figure 9). Cells  
 291 treated with the vehicle control exhibited neurite branching characterized by a broad network. While OA  
 292 did not induce any morphological modification up to 320 nM, PTX2 from 180 nM showed neurite atrophy  
 293 and decrease of body cell area.



294  
 295 **Figure 9. Morphological modifications of EGC after a 24 hrs apical treatment with PTX2 and OA.**  
 296 Evaluation of cell morphology was carried out by phase contrast microscopy. Each image is representative of  
 297 three independent experiments. A: vehicle control (5% MeOH); B: 260 nM PTX2; C: 320 nM OA. Scale bar =  
 298 100  $\mu$ m.

### 299 3.7. GDNF and iNOS levels in EGC

300 After 24 hrs of apical treatment, GDNF and iNOS protein levels were not affected by PTX2 in EGC (Figure 10).  
 301 However, a significant increase of GDNF was observed with OA, reaching 1.5-fold at 150 nM. OA induced also  
 302 iNOS increase, but not significantly, reaching 1.4-fold at the highest dose.



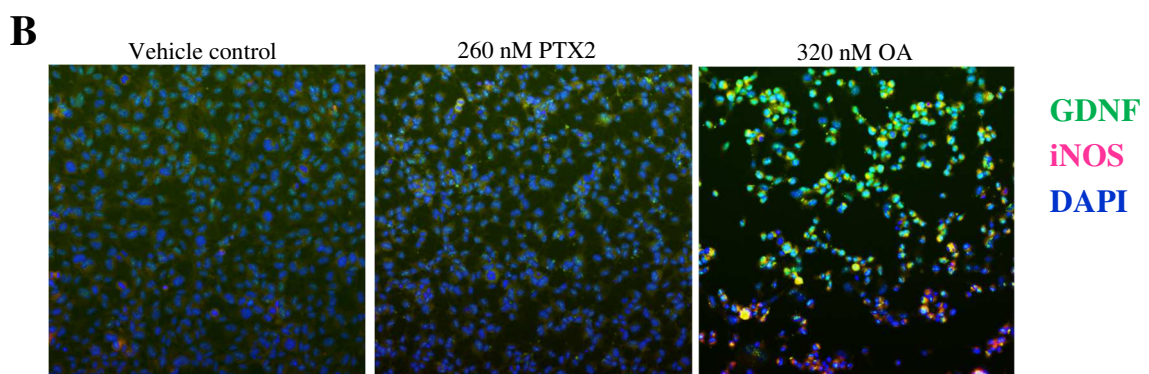
303

304

305

306

307



308

309 **Figure 10. GDNF and iNOS responses in EGC in tri-culture with Caco-2/HT29-MTX co-cultures after 24**  
 310 **hrs apical treatment with PTX2 and OA.** A: GDNF and iNOS levels were expressed as fold change compared  
 311 to the vehicle control set to 1. Values are presented as means  $\pm$  SEM. Positive control (Cytomix): 1.7-fold  
 312 ( $\pm$  0.2) for GDNF and 1.8-fold ( $\pm$  0.1) for iNOS. Three independent experiments were performed \*: value  
 313 significantly different from the vehicle control ( $P < 0.05$ ). B: GDNF (green), iNOS (purple) and nucleus (DAPI)  
 314 after 24 hrs exposure to 260 nM PTX2 and 320 nM OA were carried out by HCA. Each image is representative  
 315 of three independent experiments. Scale bar = 60  $\mu$ m.

### 316 3.8. Modulation of genes expression following treatment with PTX2 and OA on EGC

317 Additional investigations were done through expression analysis of key genes involved in viability,  
 318 inflammation and gliomediators expression for EGC (Table 2). In basolateral EGC, 150 nM PTX2 induced *IL-6*  
 319 up-regulation (5.8-fold). *BDNF* and *GDNF* gliomediator genes were up-regulated in a concentration-dependent  
 320 manner by OA, reaching 3.8-fold and 3.5-fold respectively with 175 nM OA compared to the vehicle control.

321 **Table 2. Relative gene expression of EGC in tri-culture with Caco-2/HT29-MTX co-cultures after 24 hrs**  
 322 **apical treatment with PTX2 and OA.** The analysis of gene expression was carried out by RT-qPCR. Values  
 323 are normalized to the reference gene ACTB and presented as fold changes of the vehicle control (red for  
 324 up-regulated, blue for down-regulated). Three independent experiments were performed. \*, \*\*: significantly  
 325 different from the vehicle control ( $P < 0.05$  and  $P < 0.01$  respectively).

326



327

Biological functions	Genes	PTX2 (nM)			OA (nM)		
		100	150	200	75	125	175
<b>Viability</b>	<i>BNIP3</i>						
	<i>CASP3</i>						
	<i>GABARAP</i>						
	<i>MTOR</i>						
	<i>LC3B</i>						
<b>Inflammation</b>	<i>IL6</i>		*				
	<i>MAPK8</i>						
	<i>MAPK11</i>						
	<i>MYD88</i>						
	<i>ERK1</i>						
	<i>ERK2</i>						
	<i>CCL2</i>						
<b>Gliomediator</b>	<i>BDNF</i>						*
	<i>GDNF</i>						**
	<i>S100<math>\beta</math></i>						
	<i>EGF</i>						
	<i>RAGE</i>						
	<i>TGF<math>\beta</math>1</i>						

#### 328 4. Discussion

329 In this study, a relevant tri-culture cell model that includes key cells of the human intestinal epithelium  
330 (absorptive cells, goblet cells and enteric glial cells) has been experimented for the first time in the toxicology  
331 area. As already observed (Neunlist et al., 2007 ; Van Landeghem et al., 2011 ; Xiao et al., 2011 ; Coquenlorge  
332 et al., 2016), the addition of EGC in the basal compartment increased the TEER value. Globally, our results  
333 showed that the presence of EGC could affect the response of Caco-2/HT29-MTX co-cultures after toxins  
334 exposure. Interestingly, the impact of the presence of EGC was toxin-dependent.

335 In the present study, the viability of Caco-2/HT29-MTX co-cultures decreased down to 20% after apical  
336 exposure to 260 nM PTX2. At the same time, an inflammatory response (increase of IL-8 mRNA and IL-8  
337 release) was induced. Similar results on viability and inflammation were previously obtained with PTX2 on  
338 Caco-2/HT29-MTX co-cultures without EGC (Reale et al., 2020), suggesting that the presence of EGC did not  
339 have a strong impact on these endpoints. Concerning Caco-2/HT29-MTX monolayer integrity, we observed a  
340 significant decrease of TEER values and an increase of LY permeability from 180 nM PTX2. Although  
341 numerous areas without cells were observed with the higher PTX2 concentrations, no modification of the tight  
342 junction ZO-1 protein localization was noticed. Without EGC, the disruption of Caco-2/H29-MTX monolayer  
343 integrity (TEER and LY results) was observed only from 260 nM PTX2 (Reale et al., 2020). In fact, in a glial  
344 stress environment, EGC have been documented to affect intestinal permeability through the alteration of tight  
345 junctions by the release of some gliomediators such as S100 $\beta$  and NO (Neunlist et al. 2008; Turco et al. 2014,  
346 Olson et al., 2009). Morphologically, PTX2 has been previously shown to induce neurite atrophy of EGC  
347 (Reale et al. 2019). Interestingly, in this study, we observed also such morphological alterations in EGC with an  
348 apical exposure from 180 nM PTX2. It suggests that the toxin was able to cross the Caco-2/HT29-MTX  
349 monolayer or, that EGC were affected by other components such as IL-8 released by Caco-2/HT29-MTX  
350 co-cultures in response to PTX2. Indeed, EGC have been documented to be sensitive to cytokines with the  
351 induction of morphological alterations (Rosenbaum et al. 2016; Von Boyen et al. 2006a; Von Boyen 2004).  
352 However, we did not detect PTX2 in the basal compartment (below the LOD of 25 pg/mL) (data not shown).  
353 Several hypotheses can be proposed: chemical modifications of PTX2 (biotransformation, opening of the  
354 lactone ring or conversion to the seco-acid form), efflux into the apical side or accumulation into cells.

355 In the present study, we reported a decrease of Caco-2/HT29-MTX co-cultures viability around 20% at 320 nM  
356 OA. In addition, an inflammatory response of Caco-2/HT29-MTX co-cultures through IL-8 mRNA up  
357 regulation (6-fold) and increase of IL-8 release (14-fold) was observed. At the same OA concentration but  
358 without EGC, the decrease of viability reached 32% and a larger increase of IL-8 release (28-fold) was reported  
359 (Reale et al., 2020). Cell protection of Caco-2/HT29-MTX co-cultures by the presence of EGC could be related  
360 to the up-regulation of protective gliomediators secreted by EGC in response to the huge IL-8 cytokine release.  
361 Other studies have pointed out that some factors such as inflammation could stimulate the secretion of  
362 gliomediators by EGC (Rosenbaum et al. 2016; Von Boyen 2004). Indeed, we observed an up-regulation of  
363 BDNF and GDNF mRNA strengthened by the increase of GDNF protein. These gliomediators have been  
364 documented to promote cell viability (Coelho-Aguiar et al. 2015; Neunlist et al. 2014) and to possess  
365 anti-inflammatory properties by reducing cytokines production of intestinal epithelial cells (Chow and  
366 Gulbransen 2017; Coelho-Aguiar et al. 2015; Yu and Li 2014). Similarly, *in vivo* assays in mice suffering from

367 intestinal inflammation pointed out that GDNF administration reduced inflammation (Zhang et al. 2010).  
368 Moreover, BDNF knock-out mice showed an important apoptosis of intestinal epithelial cells (Li et al., 2018;  
369 Zhao et al., 2018). Nevertheless, other gliomediators could also be involved in the reduction of IL-8 release  
370 observed in our study. Indeed, the literature reports that both GSNO and NGF gliomediators are up-regulated  
371 during inflammation and are involved in the reduction of inflammation through the decrease of cytokine  
372 production (Corti et al. 2014; Neunlist et al. 2013; von Boyen et al. 2006b).

373 Concerning the Caco-2/HT29-MTX monolayer integrity, a decrease of the TEER (around 38%) was noticed at  
374 200 nM OA in the present study but the integrity of the monolayer at this dose stayed above the acceptable limit  
375 (130 ohm.cm<sup>2</sup>). If a similar decrease of the TEER (around 40%) was also obtained without EGC, the TEER  
376 reached a value below the threshold (Reale et al., 2020) indicating seemingly a protective effect of EGC on the  
377 monolayer integrity. Regarding tight junctions, OA affected the localization of ZO-1 at 320 nM: the whole  
378 staining was reduced and some accumulation occurred on the top of the cells. At the same concentration without  
379 EGC, ZO-1 localization of Caco-2/HT29-MTX co-cultures was also perturbed and hugely redistributed into the  
380 cytoplasm, showing irregular cell borders labelling and many areas without cells. Again, it seems that EGC  
381 could prevent alterations of Caco-2/HT29-MTX co-cultures integrity probably through gliomediators  
382 production and secretion. Indeed, it has been shown that, when provoking EGC stress by a cytomix treatment  
383 (TNF $\alpha$  + IFN $\gamma$  + IL-1 $\beta$ ), the integrity of Caco-2 cells was enhanced through the release of some gliomediators  
384 (Cheadle et al., 2013; Neunlist et al., 2013; Savidge et al., 2007). GDNF has been mainly documented to  
385 strengthen the intestinal barrier by limiting the degradation of ZO-1 and occludin (Ben-Horin and Chowers  
386 2008; Langness et al. 2017; Steinkamp et al. 2003; Steinkamp et al. 2012; Xiao et al. 2014; Yu and Li 2014).  
387 Moreover, BDNF has been also implicated in the intestinal epithelium integrity (Li et al., 2018, Zhao et al.,  
388 2018).

389 In the present study, OA crossing through Caco-2/HT29-MTX monolayer reached 8% after an apical treatment  
390 of 200 nM OA, while a previous study has observed only a limited crossing of OA (2%) with the same  
391 concentration with Caco-2 cells (Ehlers et al. 2011). Since OA has been documented to be taken-up into the  
392 cells by the human transporter OATP1B3 (Ikema et al. 2015), a higher crossing value could be expected in the  
393 co-culture model due to the higher expression of this transporter in HT29-MTX cells compared to Caco-2 cells  
394 where OATP1B3 is far less expressed (Li et al. 2014). Moreover, the transporter P-gP is implicated in the apical  
395 efflux of OA by Caco-2 cells (Ehlers et al. 2014). This transporter is not expressed in HT29-MTX cells  
396 (Barlovatz-Meimom and Ronot 2014; Mahler et al. 2009), thus probably decreasing the global efflux of OA by  
397 Caco-2/HT29-MTX co-cultures compared to Caco-2 cells alone.

398 Finally, we also observed a slight decrease of EGC viability (around 20%) at the highest OA concentration.  
399 Such effect occurred concomitantly with an increase of iNOS level, hallmark feature of glial stress. In such  
400 condition, the concentration of OA in the basolateral compartment was calculated as equal to 30.6 nM. At this  
401 OA concentration, no decrease of viability on EGC alone was previously observed (Reale et al. 2019).  
402 Therefore, other compounds might contribute to the alteration of EGC viability in the present study. As OA  
403 induced a huge IL-8 release, that could be a good candidate (Von Boyen et al. 2006a; Von Boyen 2004).

## 404 5. Conclusions

405 In this study we investigated the impacts induced by PTX2 and OA exposure on an intestinal tri-culture model  
406 made of Caco-2, HT29-MTX and EGC. In conclusion, the presence of EGC did not affect the viability and the  
407 inflammation response of Caco-2/HT29-MTX co-cultures exposed to PTX2 but enhanced a decrease of the  
408 monolayer integrity. With OA, the presence of EGC increased both the survival and the integrity of  
409 Caco-2/HT29-MTX monolayers, as well as reduced their inflammatory response. The results of this study  
410 suggested that EGC of the enteric nervous system could be activated by the response of intestinal epithelial cells  
411 to phycotoxins and could be involved in preventing toxicity through the release of GDNF and BDNF  
412 gliomediators.

413

414 **Author Contributions:** Conceived and designed the experiments: O.R., A.H. and V.F. Performed the experiments:  
415 O.R and D.B. Analyzed the data: O.R., A.H. and V.F. Wrote the paper: O.R., D.B, A.H. and V.F.

416 **Conflicts of Interest:** The authors declare no conflict of interest.

417 **Acknowledgment:** We thank Angelika Hiller who carried out the LC MS-MS measurements.

418 **Funding:** This research did not receive any specific grant from funding agencies in the public, commercial, or not-for-profit  
419 sectors.

## 420 References

- 421 Alarcan J., Dubreil E., Huguet A., Hurtaud-Pessel D., Hessel-Pras S., Lampen A., Fessard V., Le Hegarat L.,  
422 2017. Metabolism of the Marine Phycotoxin PTX-2 and Its Effects on Hepatic Xenobiotic Metabolism:  
423 Activation of Nuclear Receptors and Modulation of the Phase I Cytochrome P450. *Toxins (Basel)* 9(7)  
424 doi:10.3390/toxins9070212
- 425 Alarcan J., Barbe S., Kopp B., Hessel-Pras S., Braeuning A., Lampen A., Le Hegarat L., Fessard V., 2019.  
426 Combined effects of okadaic acid and pectenotoxin-2, 13-desmethylspirolide C or yessotoxin in human  
427 intestinal Caco-2 cells. *Chemosphere* 228, 139e148.
- 428 Ares I.R., Louzao M.C., Vieytes M.R., Yasumoto T., Botana L.M., 2005. Actin cytoskeleton of rabbit intestinal  
429 cells is a target for potent marine phycotoxins. *J Exp Biol* 208(Pt 22):4345-54 doi:10.1242/jeb.01897
- 430 Barlovatz-Meimon G. and Ronot X., 2014. Culture de cellules animales-3ème ed. chapitre 27. Système intestinal  
431 Ben-Horin S. and Chowers Y., 2008 Neuroimmunology of the gut: physiology, pathology, and pharmacology.  
432 *Curr Opin Pharmacol* 8(4):490-5 doi:10.1016/j.coph.2008.07.010
- 433 Bush T.G., Savidge T.C., Freeman T.C., Cox H.J., Campbell E.A., Mucke L., Johnson M.H., Sofroniew M.V.,  
434 1998. Fulminant jejuno-ileitis following ablation of enteric glia in adult transgenic mice. *Cell*. 93,  
435 189-201.
- 436 Cheadle, G.A., Costantini, T.W., Lopez, N., Bansal, V., Eliceiri, B.P., Coimbra, R., 2013. Enteric glia cells  
437 attenuate cytomix-induced intestinal epithelial barrier breakdown. *PLoS One* 8, e69042.
- 438 Chow A.K. and Gulbransen B.D., 2017. Potential roles of enteric glia in bridging neuroimmune communication  
439 in the gut. *Am J Physiol Gastrointest Liver Physiol* 312(2):G145-G152 doi:10.1152/ajpgi.00384.2016
- 440 Coelho-Aguiar M., Bon-Frauches A.C., Gomes A.L., Pires Verissimo C., Pinheiro Aguiar D., Matias D., Bastos de  
441 Moraes Thomasi B., Souza Gomes A., Anne de Castro Brito A., Moura-Neto V., 2015. The enteric glia:  
442 identity and functions. *Glia* 63(6):921-35 doi:10.1002/glia.22795
- 443 Corti A., Franzini M., Scataglini I, Pompella A., 2014. Mechanisms and targets of the modulatory action of  
444 S-nitroglutathione GSNO on inflammatory cytokines expression. *Archives of Biochemistry and*  
445 *Biophysics* 562:80-91

- 446 Dietrich J., Grass I., Gunzel D., Herek S., Braeuning A., Lampen A., Hessel-Pras S., 2019. The marine biotoxin  
447 okadaic acid affects intestinal tight junction proteins in human intestinal cells. *Toxicol. Vitro* 58,  
448 150e160.
- 449 EFSA, 2008. Marine biotoxins in shellfish – okadaic acid and analogues , Scientific Opinion of the Panel on  
450 Contaminants in the Food chain. *EFSA Journal* 589:1-62
- 451 EFSA, 2009. Marine biotoxins in shellfish – Summary on regulated marine biotoxins1 Scientific Opinion of the  
452 Panel on Contaminants in the Food Chain. *EFSA Journal* 1309:1-23
- 453 Ehlers A., Scholz J., These A., Hessel S., Preiss-Weigert A., Lampen A., 2011. Analysis of the passage of the  
454 marine biotoxin okadaic acid through an in vitro human gut barrier. *Toxicology* 279(1-3):196-202  
455 doi:10.1016/j.tox.2010.11.001
- 456 Ehlers A., These A., Hessel S., Preiss-Weigert A., Lampen A., 2014. Active elimination of the marine biotoxin  
457 okadaic acid by P-glycoprotein through an in vitro gastrointestinal barrier. *Toxicol Lett* 225(2):311-7  
458 doi:10.1016/j.toxlet.2013.12.019
- 459 Ferron P.J., Hogeveen K., De Sousa G., Rahmani R., Dubreil E., Fessard V., Le Hegarat L., 2016. Modulation of  
460 CYP3A4 activity alters the cytotoxicity of lipophilic phycotoxins in human hepatic HepaRG cells.  
461 *Toxicol In Vitro* 33:136-46 doi:10.1016/j.tiv.2016.02.021
- 462 Ferron P.J., Hogeveen K., Fessard V., Le Hegarat L., 2014. Comparative analysis of the cytotoxic effects of  
463 okadaic acid-group toxins on human intestinal cell lines. *Mar Drugs* 12(8):4616-34  
464 doi:10.3390/md12084616
- 465 Forstner, J.F., 1994. Gastrointestinal Mucus, in *Physiology of the Gastrointestinal Tract*. R. Press, Editor,  
466 1255-1283.
- 467 Hess P., McCarron P., Rehmann N., Kilcoyne J., McMahon T., Ryan G., Ryan P.M., Twiner M.J., Doucette  
468 G.J.M.S., Ito E., Yasumoto T., 2007. Isolation and purification of azaspiracids from naturally  
469 contaminated materials, and evaluation of their toxicological effects - final project report ASTOX  
470 (ST/02/02), 28. Marine Institute - Marine Environment & Health, p. 119.
- 471 Ikema S., Takumi S., Maeda Y., Kurimoto T., Bohda S., Kingstone Chigwechokha P., Sugiyama Y., Shiozaki K.,  
472 Furukawa T., Komatsu M., 2015. Okadaic acid is taken-up into the cells mediated by human  
473 hepatocytes transporter OATP1B3. *Food Chem Toxicol* 83:229-36 doi:10.1016/j.fct.2015.06.006
- 474 Ishige M., Satoh N., Yasumoto T., 1988. Pathological studies on mice administered with the causative agent of  
475 diarrhetic shellfish poisoning (okadaic acid and pectenotoxin-2). *Hokkaidoritsu Eisei Kenkyushoho*  
476 38:15-18
- 477 Ito E., Speijers J., Fessard V., Le Hegarat L., Yasumoto T., 2004. Draft to the Joint FAO/IOC/WHO (Food and  
478 Agriculture Organization of the United Nations/ Intergovernmental Oceanographic Commission of  
479 UNESCO/ World Health Organization) ad hoc Expert Consultation on Biotoxins in Bivalve Molluscs,  
480 Oslo, Norway.
- 481 Ito E., Suzuki T., Oshima Y., Yasumoto T., 2008. Studies of diarrhetic activity on pectenotoxin-6 in the mouse  
482 and rat. *Toxicon* 51:707-716
- 483 Ito E., Yasumoto T., Takai A., Imanishi S., Harada K., 2002. Investigation of the distribution and excretion of  
484 okadaic acid in mice using immunostaining method. *Toxicon* 40:159-165
- 485 Kittler K., Fessard V., Maul R., Hurtaud-Pessel D., 2014. CYP3A4 activity reduces the cytotoxic effects of  
486 okadaic acid in HepaRG cells. *Archives of Toxicology* 88(8):1519-1526 doi:10.1007/s00204-014-1206-x

- 487 Kittler K., Preiss-Weigert A., These A., 2010. Identification Strategy Using Combined Mass Spectrometric  
488 Techniques for Elucidation of Phase I and Phase II in Vitro Metabolites of Lipophilic Marine Biotoxins.  
489 Anal Chem 82:9329-9335
- 490 Langness S., Kojima M., Coimbra R., Eliceiri B.P., Costantini T.W., 2017. Enteric glia cells are critical to limiting  
491 the intestinal inflammatory response after injury. American Journal of Physiology-Gastrointestinal  
492 and Liver Physiology 312(3):G274-G282 doi:10.1152/ajpgi.00371.2016
- 493 Li J., Zhang W., Allen S.M., Huang Y., Bode C., Owen A., Hidalgo I.J., 2014. OATP expression in human  
494 intestinal epithelial cells and its influence on the transport of statin drugs across Caco-2 cell  
495 monolayers 16th North American Regional ISSX Meeting
- 496 Li C., Cai Y.Y., Yan Z.X., 2018. Brain-derived neutrophilic factor preserves intestinal mucosal barrier function and  
497 alters gut microbiota in mice. Kaoshiung J Med Sci 34, 134-141.
- 498 Mahler G.J., Shuler M.L., Glahn R.P., 2009. Characterization of Caco-2 and HT29-MTX cocultures in an in vitro  
499 digestion/cell culture model used to predict iron bioavailability. Journal of Nutritional Biochemistry  
500 20(7):494-502 doi:10.1016/j.jnutbio.2008.05.006
- 501 Moriez R., Abdo H., Chaumette T., Faure M., Lardeux B., Neunlist M., 2009. Neuroplasticity and  
502 neuroprotection in enteric neurons: role of epithelial cells. Biochem Biophys Res Commun  
503 382(3):577-82 doi:10.1016/j.bbrc.2009.03.073
- 504 Neunlist M., Rolli-Derkinderen M., Latorre R., Van Landeghem L., Coron E., Derkinderen P., 2014. Enteric glial  
505 cells: recent developments and future directions. Gastroenterology 147(6):1230-7  
506 doi:10.1053/j.gastro.2014.09.040
- 507 Neunlist M., Van Landeghem L., Bourreille A., Savidge T., 2008. Neuro-glial crosstalk in inflammatory bowel  
508 disease. J Intern Med 263(6):577-83 doi:10.1111/j.1365-2796.2008.01963.x
- 509 Neunlist M., Van Landeghem L., Mahe M.M., Derkinderen P., des Varannes S.B., Rolli-Derkinderen M., 2013.  
510 The digestive neuronal-glia-epithelial unit: a new actor in gut health and disease. Nat Rev  
511 Gastroenterol Hepatol 10(2):90-100 doi:10.1038/nrgastro.2012.221
- 512 Ochoa-Cortes F., Turco F., Linan-Rico A., Soghomonyan S., Whitaker E., Wehner S., Cuomo R., Christofi F.L.,  
513 2016. Enteric glial cells : a new frontier in neurogastroenterology and clinical target for inflammatory  
514 bowel diseases. Inflamm Bowel Dis 22, 433-449.
- 515 Olson N., Greul A.K., Hritova M., Bove P.F., Kasahara D.I., Van der Vliet A., 2009. Nitric oxide and epithelial  
516 barrier function : regulation of tight junction proteins and epithelial permeability. Arch Biochem  
517 Biophys 484, 205-213.
- 518 Reale O., Huguet A., Fessard V., 2019. Novel Insights on the Toxicity of Phycotoxins on the Gut through the  
519 Targeting of Enteric Glial Cells. Mar Drugs 17(7) doi:10.3390/md17070429
- 520 Reale O., Huguet A., Fessard V., 2020 Co-culture model of Caco-2/HT29-MTX cells : A promising tool for  
521 investigation of phycotoxins toxicity on the intestinal barrier. Chemosphere. Article in Press.
- 522 Reguera B., Riobo P., Rodriguez F., Diaz P.A., Pizarro G., Pas B., Franco J.M., Blanco J., 2014. Dinophysis toxins:  
523 causative organisms, distribution and fate in shellfish. Mar Drugs 12(1):394-461  
524 doi:10.3390/md12010394
- 525 Rosenbaum C., Schick M.A., Wollborn J., Heider A., Scholz C.J., Cecil A., Niesler B., Hirrlinger J., Walles H.,  
526 Metzger M., 2016. Activation of Myenteric Glia during Acute Inflammation In Vitro and In Vivo. PLoS  
527 One 11(3):e0151335 doi:10.1371/journal.pone.0151335

- 528 Savidge, T.C., Newman, P., Pothoulakis, C., Ruhl, A., Neunlist, M., Bourreille, A., Hurst, R., Sofroniew, M.V.,  
529 2007. Enteric glia regulate intestinal barrier function and inflammation via release of  
530 S-nitrosoglutathione. *Gastroenterology* 132, 1344-1358.
- 531 Steinkamp M., Geerling I., Seufferlein T., Von Boyen G., Egger B., Grossmann J., Ludwig L., Adler G.,  
532 Reinshagen M., 2003. Glial-derived neurotrophic factor regulates apoptosis in colonic epithelial cells.  
533 *Gastroenterology* 124(7):1748-1757 doi:10.1016/s0016-5085(03)00404-9
- 534 Steinkamp M., Gundel H., Schulte N., Spaniol U., Pflueger C., Zizer E., Von Boyen G., 2012. GDNF protects  
535 enteric glia from apoptosis: evidence for an autocrine loop. *BMC Gastroenterol* 12:6  
536 doi:10.1186/1471-230X-12-6
- 537 Suzuki T., Walter J.A., LeBlanc P., MacKinnon S., O Miles C., Wilkins A.L., Munday R., Beuzenberg V.,  
538 MacKenzie A.L., Jensen D.J., Cooney J.M., Quilliam M.A., 2006. Identification of pectenotoxin-11 as  
539 34S-hydroxypectenotoxin-2, a new pectenotoxin analogue in the toxic dinoflagellate *Dinophysis acuta*  
540 from New Zealand. *Chemical Research in Toxicology* 19(2):310-319
- 541 Tarantini A., Lancelleur R., Mourot A., 2015. Toxicity, genotoxicity and proinflammatory effects of amorphous  
542 nanosilica in the human intestinal Caco-2 cell line. *Toxicol In Vitro* 29(2):398-407  
543 doi:10.1016/j.tiv.2014.10.023
- 544 Terao K., Ito E., Managi T., Yasumoto T., 1986. Histopathological studies on experimental marine toxin  
545 poisoning. I. Ultrastructural changes in the small intestine and liver of suckling mice induced by  
546 dinophysistoxin-1 and pectenotoxin-1. *Toxicon* 24(11-12):1141-1151
- 547 Turco F., Sarnelli G., Cirillo C., Palumbo I., De Giorgi F., D'Alessandro A., Cammarota M., Giuliano M., Cuomo  
548 R., 2014. Enteroglial-derived S100B protein integrates bacteria-induced Toll-like receptor signalling in  
549 human enteric glial cells. *Gut* 63(1):105-115 doi:10.1136/gutjnl-2012-302090
- 550 Von Boyen G.B., Schulte N., Pflueger C., Spaniol U., Hartmann C., Steinkamp M., 2011. Distribution of enteric  
551 glial and GDNF during gut inflammation. *BMC Gastroenterology* 11(3):1-8
- 552 Von Boyen G.B., Steinkamp M., Geerling I., Reinshagen M., Schafer K.H., Adler G., Kirsch J., 2006a.  
553 Proinflammatory cytokines induce neurotrophic factor expression in enteric glia: a key to the  
554 regulation of epithelial apoptosis in Crohn's disease. *Inflamm Bowel Dis* 12(5):346-54  
555 doi:10.1097/01.MIB.0000219350.72483.44
- 556 Von Boyen G.B., Steinkamp M., Reinshagen M., Schafer K.H., Adler G., Kirsch J., 2006b. Nerve growth factor  
557 secretion in cultured enteric glia cells is modulated by proinflammatory cytokines. *J Neuroendocrinol*  
558 18(11):820-5 doi:10.1111/j.1365-2826.2006.01478.x
- 559 Von Boyen G.B., 2004. Proinflammatory cytokines increase glial fibrillary acidic protein expression in enteric  
560 glia. *Gut* 53(2):222-228 doi:10.1136/gut.2003.012625
- 561 Wang J., Wnag Y.Y., Lin L., Gao Y., Hong H.S., Wang D.Z., 2012. Quantitative proteomic analysis of okadaic  
562 acid treated mouse small intestines reveals differentially expressed proteins involved in diarrhetic  
563 shellfish poisoning. *Journal of Proteomics* 75:2023-2052 doi:10.1016/j.jprot.2012.01.010
- 564 Xiao W., Wang W., Chen W., Sun L., Li X., Zhang C., Yang H., 2014. GDNF is involved in the barrier-inducing  
565 effect of enteric glial cells on intestinal epithelial cells under acute ischemia reperfusion stimulation.  
566 *Mol Neurobiol* 50(2):274-89 doi:10.1007/s12035-014-8730-9
- 567 Yu Y.B. and Li Y.Q., 2014. Enteric glial cells and their role in the intestinal epithelial barrier. *World J*  
568 *Gastroenterol* 20(32):11273-11280 doi:10.3748/wjg.v20.i32.11273

- 569 Zhao D.Y., Zhang W.X., Qi Q.Q., Long X., Li X., Yu Y.B., Zuo X.L., 2018. Brain-derived neurotrophic factor  
570 modulates intestinal barrier by inhibiting intestinal epithelial cells apoptosis in mice. *Physiol Res* 67,  
571 475-485.
- 572 Zhang D.K., He F.Q., Li T.K., Hua Pang X., Xie Q., Huang X.L., Gan H.T., 2010. Glial-derived neurotrophic factor  
573 regulates intestinal epithelial barrier function and inflammation and is therapeutic for murine colitis. *J*  
574 *Pathol* 222(2):213-22 doi:10.1002/path.2749